

# Deep Expander Networks: Efficient Deep Networks from Graph Theory

Ameya Prabhu    Girish Varma    Anoop Namboodiri  
 Center for Visual Information Technology  
 Kohli Center on Intelligent Systems  
 IIIT-Hyderabad, India

ameya.prabhu@research.iiit.ac.in, {girish.varma,anoop}@iiit.ac.in

## Abstract

Deep Neural Networks, while being unreasonably effective for several vision tasks, have their usage limited by the computational and memory requirements, both during training and inference stages. Analyzing and improving the connectivity patterns between layers of a network has resulted in several compact architectures like GoogleNet, ResNet and DenseNet-BC. In this work, we utilize results from graph theory to develop an efficient connection pattern between consecutive layers. Specifically, we use expander graphs that have excellent connectivity properties to develop a sparse network architecture, the deep expander network (X-Net). The X-Nets are shown to have high connectivity for a given level of sparsity. We also develop highly efficient training and inference algorithms for such networks. Experimental results show that we can achieve the similar or better accuracy as DenseNet-BC with two-thirds the number of parameters and FLOPs on several image classification benchmarks. We hope that this work motivates other approaches to utilize results from graph theory to develop efficient network architectures.

## 1. Introduction

Convolutional Neural Networks (CNNs) achieve state-of-the-art results in a variety of computer vision applications. However, they are also computationally intensive, and consume a large amount of power and runtime memory. After the success of VGG Networks [40], there has been significant interest in compressing neural networks, due to its practical value in real world use cases. However, CNNs suffer from significant redundancies in parameterization [12, 13] and often encode highly correlated parameters. Many explicit matrix compression techniques were developed, including weight pruning [28, 18, 3, 31] and quantization [15, 4, 17, 49]. In the following years, novel architecture designs that have inherently fewer parameters, while retaining good representational power [44, 19, 24] were in-

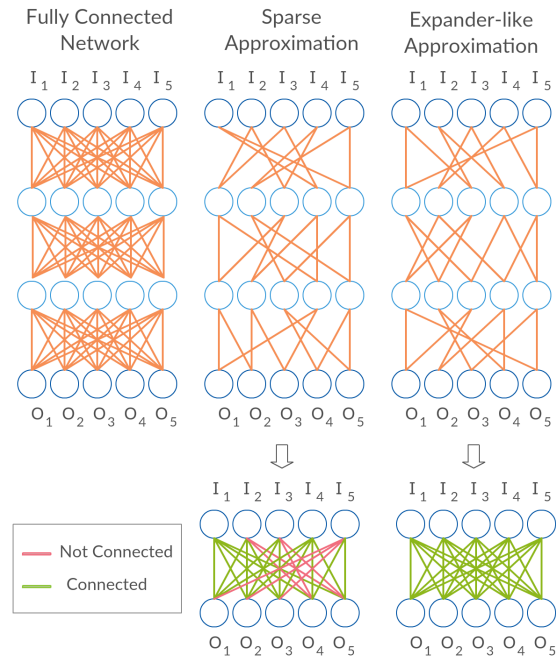


Figure 1: Popular sparse approximations are agnostic to the global information flow in a network, creating possible disconnected components. In contrast, expander graph-based models produce sparse yet highly connected networks.

troduced.

An interesting approach to designing efficient layers was to represent the connections between layers compactly. Some efficient designs of convolutional layers were obtained by using depthwise separable convolutions [6, 22, 55], dilated convolutions [52], and perforated convolutions [14] among others. More structured approaches were adopted for fully-connected layers, modeling them as Kernels [10, 47, 7] and developing structured efficient linear layers (SELLs) [5, 34, 50]. Another set of approaches use low-rank approximations [38, 49, 13] like SVD to compress linear layers. However, most of these approaches require strong assumptions such as the weight matrices being

low-rank or diagonal in the Fourier or spatial domains.

For various computer vision tasks, it is essential that the global information flows are aggregated efficiently. That is, each output node must have the capacity to be sensitive to changes from every input pixel. As we can see from Fig. 1, traditional model compression techniques such as pruning can aggravate the problem, since they can prune the neuron connections of a layer, while being agnostic of global connectivity of the network. A necessary condition for having good representational power is efficient information flow through the network, which is particularly suited to be modeled by graphs. Graphs are a versatile and effective way to model a wide range of structural representations ranging from computer networks and computational flows over time to social media and human languages.

We propose to make the connections between neurons (filters in the case of CNNs) according to specific graph constructions that are sparse and known to have good connectivity properties. The graph constructions we use are known as expander graphs, which have been widely studied in spectral graph theory [41] and pseudorandomness [45]. Expander graphs have a long history in theoretical computer science, also being used in practice in computer networks, constructing error correcting codes, and in cryptography (for a survey, see [21]). The proposed architecture, called Deep Expander Networks (X-Nets), has connections defined by an expander graph. We empirically show that X-Nets preserve the accuracy obtained using original models, while significantly reducing the number of parameters required (see Section 5.4). The structured sparsity in the expander constructions allows for fast convolution algorithms (see Section 4).

**Main Contributions:** i.) We propose to represent neuronal connections in deep networks using expander graphs. This results in networks with strong connectivity properties (Theorem 3), which are necessary to ensure good expressive power. ii.) We provide memory-efficient implementations of Linear (X-Linear) and Convolutional (X-Conv) layers using sparse matrices, with connections that form an expander graph. We further exploit the structured sparsity in the expander constructions to design fast algorithms. iii.) We empirically show that X-Nets achieve accuracies comparable to state-of-the-art networks like DenseNet-BC with two-thirds the number of parameters and FLOPs on several image classification benchmarks iv.) Efficient layer design also allows us to train wider and deeper networks frugally. Specifically for DenseNet on CIFAR datasets, the deeper models outperform the shallower ones with merely 60% the parameters.

## 2. Related Work

Previous works have taken various directions in modeling neural networks, broadly categorized into two classes:

i) Explicit matrix compression techniques such as pruning and quantization, and ii) Efficient layer designs such as Inception, residual connections and SELLS.

### 2.1. Explicit Matrix Compression Techniques

Several methods have been introduced to compress pre-trained networks. These models are typically based on low-rank decomposition [38, 36, 33] and network pruning [3, 31, 20, 35], and aim to eliminate redundant parameters and leverage the original pre-trained models [4]. There is a major body of work that quantizes the networks to achieve efficiency [37, 9, 17, 48, 2, 58, 57]. Works in train-time network pruning have explored the problem of pruning weights [46, 29] primarily from weight-level [27, 39, 42, 16] to channel-level pruning [32, 29, 46]. Weight-level pruning has the highest compression rate while channel-level pruning is easier to practically exploit and has compression rates almost on par with the former. Hence, channel-level pruning is currently considered superior [32]. Channel-level pruning approaches started out with no guidance for sparsity [4] and eventually added constraints [43, 56, 51], tending towards more structured pruning. Our method takes a different, theoretically grounded approach towards exploiting channel-level sparsity. It moves from constrained pruning to initializing the network with a well-researched sparse expander graph structure.

Explicit matrix compression techniques have three major limitations. First, the training step has to deal with the bulky full model, limiting the range of models that can be compressed. In contrast, X-Nets can possibly train significantly deeper and wider networks. Second, these approaches obtain the compressed network only after training procedure, typically achieving compactness and efficiency during test-time. X-Nets by definition are compact and runtime-efficient even while training. Third, matrix compression require multiple phases of training, followed by re-training, to identify the important connections and allow the unpruned connections to adjust for the previously pruned connections. In the case of quantization, they often require both quantized and original models in memory at train-time. In contrast, we start with an explicitly sparse topology that has good connectivity properties, requiring only a single training phase as when training the original models.

### 2.2. Efficient Layer Designs

Many works have tried to compress models by designing compact blocks of layers. Replacing fully connected layers with global average pooling [30], developing novel convolutional block architectures [44, 24, 22], and introducing residual connections [19]. This enables the training of compact, but accurate deep networks [19, 54, 23]. This motivated several works that construct efficient layer designs [22, 6] by introducing structures to model the connections

between the layers, modeling the weight matrices as kernels [7, 47] and developing SELLS [50, 34, 4]. Many works make strong assumptions like the matrix being low-rank [38], or the matrix being efficiently modeled as a diagonal matrix in the Fourier or spatial domain [50, 34, 4]. Unlike their approach, which models only fully connected layers, we can model convolutional layers as well. Hence, we can apply our method to model connections between neurons in the convolutional layers of various compact but accurate layer designs like ResNet and DenseNet.

### 3. Approach

We propose to model connections between neural network layers, using specific graphs called Expanders, which are known to have good connectivity properties (for a detailed survey, see [21]). In this section, we give the relevant definitions, and state the connectivity properties of expander graphs. We then proceed to give the construction of linear and convolutional layers defined by an expander graph, and formally prove that these layers have good sensitivity properties.

#### 3.1. Expander Graphs

A bipartite expander with degree  $D$  and spectral gap  $\gamma$ , is a bipartite graph  $G = (U, V, E)$  ( $E$  is the set of edges,  $E \subseteq U \times V$ ) in which:

**Sparsity:** Every vertex in  $V$  has only  $D$  neighbors in  $U$ . We will be using constructions with  $D \ll |U|$ . Hence the number of edges is only  $D \times |V|$  as compared to  $|U| \times |V|$  in a dense graph.

**Spectral Gap:** The second largest eigenvalue in absolute value  $\lambda$  of the adjacency matrix is bounded away from  $D$  (the largest eigenvalue). Formally  $1 - \lambda/D \geq \gamma$ .

**Properties.** Expander graphs have the following connectivity properties, efficiently modeling the connectivity pattern of neurons in a deep network (see [45], for the proofs). These properties are used to prove the sensitivity and connectivity properties of X-Nets (see Section 3.3).

**Expansion:** For every subset  $S \subseteq V$  of size  $\leq \alpha|V|$  ( $\alpha \in (0, 1)$  depends on the construction), let  $N(S)$  be the set of neighbors. Then  $|N(S)| \geq K|S|$  for  $K \approx D$ . That is, the neighbors of the vertices in  $S$  are almost distinct.

**Small Diameter:** The diameter of a graph is the length of the longest path among all shortest paths. That is, let  $l(u, v)$  be the length of the shortest path from  $u$  to  $v$ . Then the diameter  $d := \max_{u,v} l(u, v)$ . If  $G(U, V, E)$  is a  $D$ -regular expander with expansion factor  $K > 1$  and diameter  $d$ , then  $d \leq O(\log n)$ . This bound on the diameter implies that for any pair of vertices, there is a path of length  $O(\log n)$  in the graph.

**Mixing of Random Walks:** Random walks in the graph quickly converge to the uniform distribution. If we start

from any vertex and keep moving to a random neighbor, in  $O(\log n)$  steps the distribution will be close to uniform over the set of vertices.

**Constructions.** We define the specific expander graphs that will be used for the construction of X-Nets.

**Random expanders:** A random bipartite expander of degree  $D$  on vertex sets  $U, V$ , is a graph in which for every vertex  $v \in V$ , the  $D$  neighbors are chosen independently and uniformly from  $U$ . It is a well known result in graph theory that such graphs have expansion factor  $K \approx D$  (see Theorem 4.4 in [45]).

**Explicit expanders:** We also use explicit expander constructions that are obtained using the theory of finite fields. We use these constructions to give faster algorithms for training and inference. In these constructions the vertex set  $V$  is a power of some finite field, which for simplicity can be assumed to be  $\{0, 1\}^n$  (commonly known as Cayley expander. See [1]). Consider the binary string representation corresponding to the index of the vertex. Let  $H \subset \{0, 1\}^n$  be a set of generators of the group  $\{0, 1\}^n$  under XOR operation. Then the edges are of the form  $(v, v + g)$  for  $v \in \{0, 1\}^n$  and  $g \in H$ . The main advantage of explicit expanders is that we can iterate over the  $D$  neighbors of the vertex efficiently. This property helps us to design fast algorithms for explicit expanders. A more detailed construction can be found in the Appendix. The experiments are mostly performed using random expanders as they are sufficient to illustrate the power of the approach.

#### 3.2. Deep Expander Networks (X-Nets)

We give constructions of deep networks that have connections defined by an expander graph.

**Expander Linear Layer (X-Linear):** Given a bipartite expander  $G$  with degree  $D$ , the Expander Linear (X-Linear) layer defined by  $G$ , is a layer with  $|U|$  input neurons,  $|V|$  output neurons and each output neuron  $v \in V$  is only connected to the  $D$  neighbors given by  $G$ . Note that this layer has only  $|V| \times D$  parameters as compared to  $|V| \times |U|$ , which is the size of the typical linear layers. The expander graphs that we use have values of  $D \ll |U|$ , while having an expansion factor of  $K \approx D$ , which ensures that the layer still has good expressive power.

An Expander Linear Network (Linear X-Net) given by expander graphs  $G_1 = (V_0, V_1, E_1), G_2 = (V_1, V_2, E_2), \dots, G_t = (V_{t-1}, V_t, E_t)$ , is a  $t$  layer deep network in which the linear layers are replaced by X-Linear layers defined by the corresponding graphs. The total number of parameters in such a module is  $\sum_{i=1}^t D \times |V_i| \ll \sum_{i=1}^t |V_{i-1}| \times |V_i|$ .

**Expander Convolutional Layer (X-Conv):** The Expander Convolutional (X-Conv) layer defined by  $G$  is a convolutional layer with a window size of  $c \times c$ , that takes a

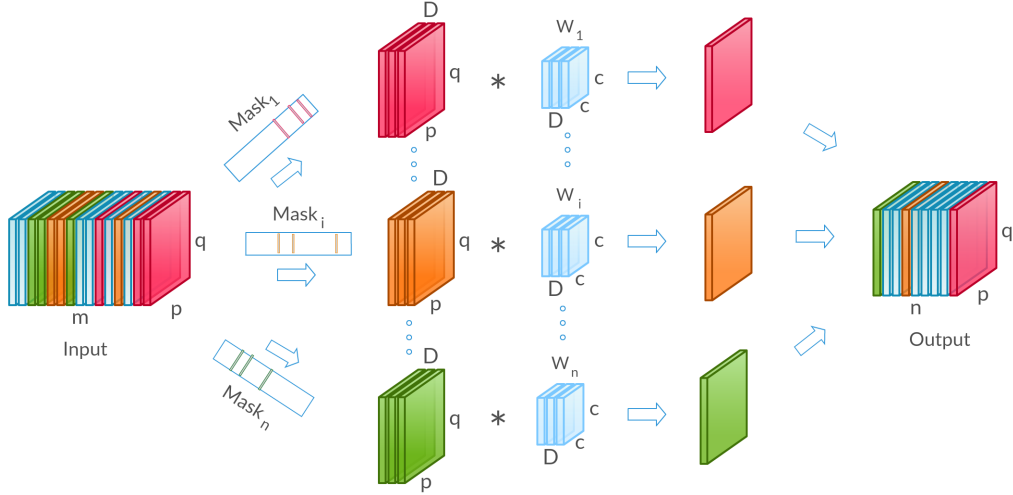


Figure 2: The proposed fast convolution algorithm for X-Conv layer. We represent all the non-zero filters in the weight matrix of the X-Conv layer in a compressed dense matrix of  $D$  channels. The algorithm starts by selecting  $D$  channels from input (with replacement) using an explicit method or by using random mask created while initializing the model. The output is computed by convolving these selected channels with the compressed weight matrices.

3D input with  $|U|$  channels and produces a 3D output with  $|V|$  channels. The output channel corresponding to a vertex  $v \in V$  is computed only using the  $D$  input channels corresponding to the neighbors of  $v$ . Hence the kernel of this X-Conv layer has  $|V| \times D \times c \times c$  parameters as compared to  $|V| \times |U| \times c \times c$ , which is the number of parameters in a vanilla CNN layer.

Similarly, given expander graphs  $G_1 = (V_0, V_1, E_1), G_2 = (V_1, V_2, E_2), \dots, G_t = (V_{t-1}, V_t, E_t)$ , the Expander Convolutional Network (Convolutional X-Net or simply X-Net) defined by them is a  $t$  layer deep network in which the convolutional layers are replaced by X-Conv layers defined by the corresponding graphs. The total number of parameters in such a module is  $t \times D \times (\sum_{i=1}^t |V_i|) \times c \times c$ .

### 3.3. Connectivity in X-Nets

X-Nets have multiple layers, each of which have connections derived from an expander graph. We can guarantee that the output nodes in such a network are sensitive to all the input nodes. Though the theorem below is proved for X-Linear Networks, it also holds for Convolutional X-Nets.

**Theorem 1** (Sensitivity of X-Nets). *Let  $n$  be the number of input as well as output nodes in the network and  $G_1, G_2, \dots, G_t$  be  $D$  regular bipartite expander graphs with  $n$  nodes on both sides. Then every output neuron is sensitive to every input in a Deep X-Linear Network defined by  $G_i$ 's with depth  $t = O(\log n)$ .*

*Proof.* For every pair of input and output  $(u, v)$ , we show that there is a path in the X-Linear network. The proof is essentially related to the fact that expander graphs have diameter  $O(\log n)$ . A detailed proof can be found in the Appendix.  $\square$

Next, we show a much stronger connectivity property known as mixing for the X-Nets. The theorem essentially says that the number of paths between subsets of input and output nodes is proportional to the product of their sizes. This result implies that the connectivity properties are uniform across all nodes as well as subsets of nodes of the same size. Hence, all nodes tend to have equally rich representational power.

**Theorem 2** (Mixing in Deep Expander Networks). *Let  $n$  be the number of input as well as output nodes in the network and  $G_1, G_2, \dots, G_t$  be  $D$  regular bipartite expander graphs with  $n$  nodes on both sides. Let  $S, T$  be subsets of input and output nodes in the X-Linear Network defined by the  $G_i$ 's. The number of paths between  $S$  and  $T$  is  $\approx D|S||T|/n$ .*

*Proof.* Detailed proof is provided in the Appendix.  $\square$

## 4. Implementation

In this section, we give some implementations of X-Linear and X-Conv layers. Our implementation gives speed ups in inference as well as in the training phase. Also, we exploit the structured sparsity of explicit expanders to design fast algorithms, especially for X-Conv layers. We propose two methods of training X-Nets, both requiring substantially less memory and computational cost: 1) Using Sparse Representations 2) Expander-Specific Fast Algorithms.

### 4.1. Using Sparse Representation

The adjacency matrices of random expanders as well as explicit expanders are highly sparse for  $D \ll n$ . Hence, we can initialize a sparse matrix with non-zero entries corresponding to the edges of the expander graphs. This is possible

---

**Algorithm 1 Fast Convolution Algorithm**Fast Algorithm for Convolutions in X-Conv Layer

---

- 1: Initialization
  - 2: For every vertex  $v \in \{1, \dots, n\}$ , let  $N(v, i)$  denote the  $i$ th neighbor of  $v$  ( $i \in \{1, \dots, D\}$ ).
  - 3: Let  $K_v$  be the  $c \times c \times D \times 1$  sized kernel associated with the  $v$ th output channel.
  - 4: Let  $O_v[x, y]$  be the output value of the  $v$ th channel at the position  $x, y$ .
  - 5: **for**  $v=1$  to  $n$  **do**
  - 6:    $O_v[x, y] = K_v * \text{Mask}_{N(v,1), \dots, N(v,D)}(I)[x, y]$
- 

since the sparse points are pre-initialized and never change, unlike in most pruning techniques. Sparse matrix representations are easy to implement, and can be supported by most deep learning libraries.

## 4.2. Expander-Specific Fast Algorithms

Next, we present fast algorithms that exploit the structured sparsity of explicit expanders. Moreover, our algorithm for X-Conv layers works for random expanders as well.

**X-Conv:** In an X-Conv layer, every output channel is only sensitive to some  $D$  input channels. These channels are chosen randomly in random expanders, while it is obtained by XOR operations on the index of the output channels for explicit expanders. We propose to use a mask to select  $D$  channels of the input, and then convolve with a  $c \times c \times D \times 1$  kernel, obtaining a single channel per filter in the output. Though this operation has to be done for each output channel, all the operations can be done in parallel. Moreover, the masking out operations can be optimized in case of explicit expanders. This can be done by efficiently iterating over the neighbors of a vertex in explicit expanders (see Algorithm 1). This is illustrated in Figure 2.

**X-Linear:** The sparse algorithms for X-Linear layers require efficient sparse matrix algorithms. However, for explicit expanders we can show that the X-Linear layers defined by them have a fast algorithm defined in terms of vanilla dense matrix operations. Let  $h_1, \dots, h_D$  be some generators of the group  $\{0, 1\}^n$  used for the explicit expander construction. We can create a fixed mapping from these generators to  $\{1, \dots, D\}$ . The mapping can be used to store the weights of the X-Linear layer as an  $N \times D$  dense matrix where  $N$  is the output size. The  $i, j$ th entry of the matrix represents the weight assigned to the  $j$ th connection of the  $i$ th neighbor. The algorithm first rearranges the input of size  $m$  to a matrix of dimension  $N \times D$ . The  $(i, j)$ th entry of the matrix is the value of the input at the  $j$ th neighbor of the  $i$ th vertex. Then it performs coordinate-wise multiplication with the weights matrix and finally sums up the operation over the second axis (see Algorithm 2).

---

**Algorithm 2 Fast Linear Algorithm**Fast Algorithm for the X-Linear Layer using Explicit Expanders

---

- 1: Initialization
  - 2: For every neuron output  $v \in \{1, \dots, n\}$ , let  $N(v, i)$  denote the  $i$ th neighbor of  $v$  ( $i \in \{1, \dots, D\}$ ).
  - 3: Rearrange input  $I$  of dimension  $m$  into a  $n \times D$  matrix  $I'$  such that  $I'[i, j]$  has the value of the  $j$ th neighbor of the  $i$  vertex.
  - 4: Compute  $I' * W$
  - 5:  $O_v = \sum_u (I' * W)[v, u]$
- 

## 5. Experiments

We now demonstrate the effectiveness of our proposed method on several benchmark architectures and datasets. We show that our approach is robust and can be used on different types of CNN architectures.

### 5.1. Datasets

**CIFAR-10/100** [25]: The two CIFAR datasets consist of natural images of resolution 32x32. They are subsets of the 80 Million Tiny Images dataset, with CIFAR-10 consisting of 10 classes and CIFAR-100 consisting of a more fine grained division into 100 classes. The train and test sets contain 50,000 and 10,000 images respectively. Standard data augmentation (flipping and translation) along with normalization is applied to inputs while training.

**ImageNet** [11]: ImageNet is the benchmark dataset for evaluating image recognition tasks, with over a million training images and 50,000 validation images. We resize the images to 256 x 256. Standard data augmentation (flipping and translation) along with normalization is applied to inputs while training. We report the single-center-crop validation errors of the final models.

### 5.2. Models

To demonstrate the effectiveness of our method, we build upon current state-of-the-art models and compare with previous bodies of work. We train older VGG16 models on the CIFAR-10 dataset [25], and AlexNet [26] on ImageNet [11], and benchmark the effectiveness of our method against previous state-of-the-art compression techniques.

**AlexNet** [26]: On the ImageNet[11] dataset, we compare our technique with state-of-the-art compression techniques by modeling connections using AlexNet as the base model and training two X-AlexNet networks. We explain the detailed structure of our networks in a layer-wise fashion in the Appendix.

**VGG16** [40]: We use the VGG16 as the base model to train two X-VGG16 networks on CIFAR-10. We explain

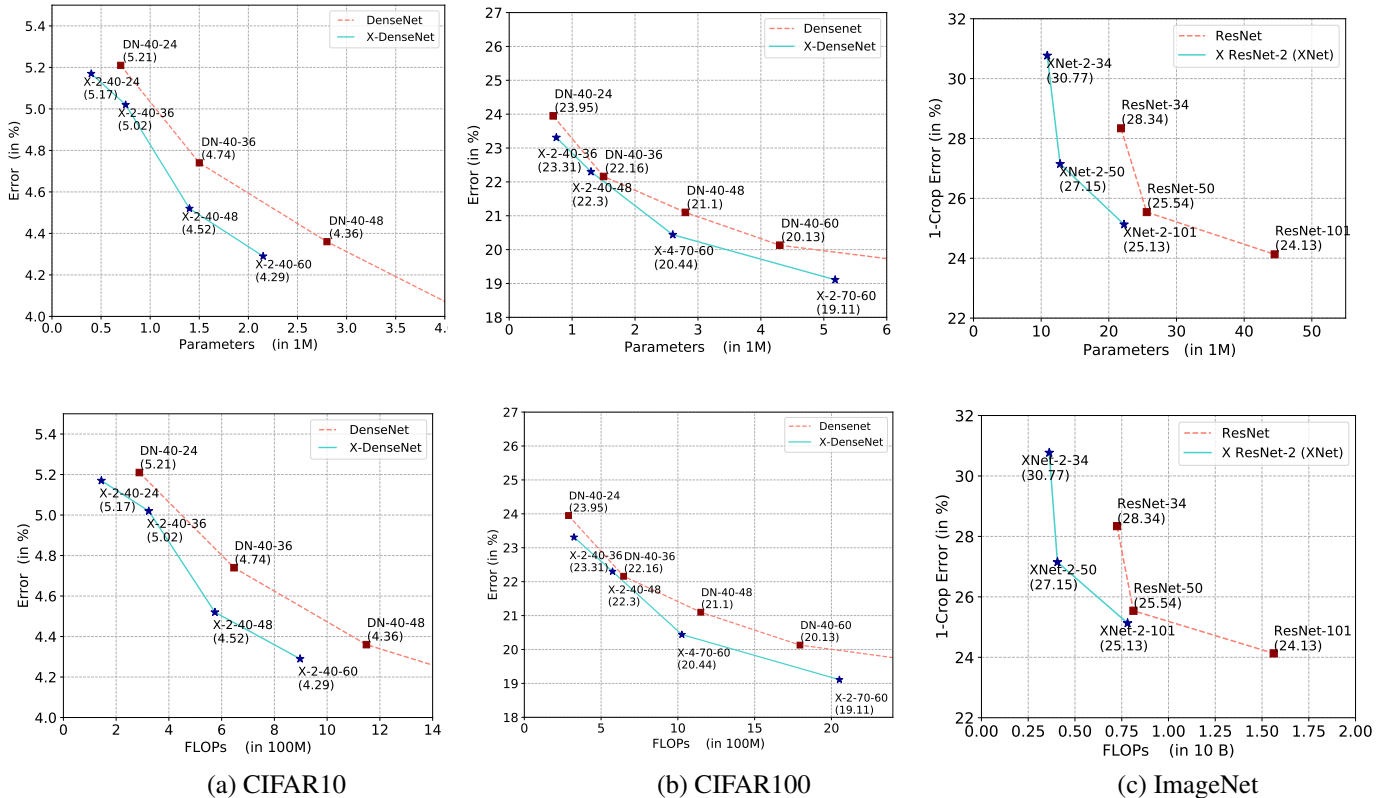


Figure 3: We show the error as a function of learned parameters (above) and FLOPs during test-time (below) for DenseNet BC [23] and ResNets [19] with X-Nets on CIFAR10, CIFAR100 and ImageNet datasets. For each datapoint, we mention the X-C-D-G notation (see Section 5.2) along with the accuracy.

the detailed structure of our networks in a layer-wise fashion in the Appendix.

We then proceed to use Expander Graphs to model connections in state-of-the-art architectures such as DenseNets and ResNets on the CIFAR-10 and ImageNet datasets. We define our X-Nets by replacing every layer in the network except the first and last with X-Conv layers.

**ResNets [19]:** We train X-ResNets for various depths and growth rates. Our X-ResNet-C-D is a  $D$  layered ResNet that has every layer except the first and last replaced by an X-Conv layer that compresses connections between it and the previous layer by a factor of  $C$ . We use ResNets-34,50,101 as base models on ImageNet dataset. Resnet-50 and 101 have the bottleneck architecture, yet our technique is able to compress them unlike previous work [32].

**DenseNets [23]:** We train X-DenseNets for various depths and growth rates. Our X-DenseNet-BC-C-D-G architecture has depth  $D$ , and growth rate  $G$ . This network has every layer except the first and last replaced by an X-Conv layer that compresses connections between it and the previous layer by a factor of  $C$ . We use DenseNet-BC-121-32,169-32,161-48,201-32 as base models on ImageNet and DenseNet-BC-40-24 to Densenet-BC-40-60 in steps of

12, along with Densenet-BC-70-60 additionally for CIFAR-100. All experiments are performed on the most efficient (DenseNet-BC) architectures. Hereon, we mean DenseNet-BC architectures as DenseNets.

Additional details regarding all models, accuracies, and numbers of parameters and FLOPs shown in Figure 3 and otherwise are tabulated in the Appendix for reference due to lack of space. Additionally, all training and testing codes, with pre-trained models, will be made available alongside the published paper for more clarity at

<http://cvit.iiit.ac.in/projects/xnet/>

### 5.3. Experimental Details

To ensure better reproducibility, we use the same hyper-parameters, models, training schedules and dataset structures from the official PyTorch repository<sup>1</sup> for ImageNet experiments. Likewise, we follow the densenet-pytorch repository by Andreas Veit<sup>2</sup> for all DenseNet-BC experiments on CIFAR-10/100 datasets, and the pytorch-vgg-cifar10 repository by Cheng-Yang Fu<sup>3</sup> for VGG16 experiments on the

<sup>1</sup><https://github.com/pytorch/examples/blob/master/imagenet/main.py>

<sup>2</sup><https://github.com/andreasveit/densenet-pytorch/>

<sup>3</sup><https://github.com/chengyangfu/pytorch-vgg-cifar10>

Method	Accuracy	#Params	Training Speedup ?
Li <i>et al.</i> [29]	93.4%	5.4M	✗
Liu <i>et al.</i> [32]	93.8%	2.3M	✗
X-VGG16-1	93.6%	1.65M (9x)	✓
X-VGG16-2	93.2%	1.15M (13x)	✓
VGG16-Orig [40]	93.7%	15.0M	-

Table 1: Comparison with other methods on CIFAR-10 dataset using VGG16 as the base model. We significantly outperform others, achieving similar accuracies with 13x compression rate.

Method	Accuracy	#Params	Training Speedup?
Network Pruning			
Collins <i>et al.</i> [8]	55.1%	15.2M	✗
Zhou <i>et al.</i> [56]	54.4%	14.1M	✗
Network Pruning [17]	57.2%	6.7M	✗
Deep Compression [17]	57.2%	6.7M	✗
GreBdec [53]	57.2%	6M	✗
Srinivas <i>et al.</i> [43]	56.9%	5.9M	✗
Guo <i>et al.</i> [16]	56.9%	3.4M	✗
SELLs			
Finetuned SVD 2 [50]	56.0%	23.4M	✓
Circulant CNN 2 [5]	56.8%	17M	✓
Adaptive Fastfood-16 [50]	57.1%	16.4M	✓
ACDC [34]	56.5%	9.7M	✓
Expanders (Ours)			
X-AlexNet-1	55.8%	9.7M	✓
X-AlexNet-2	54.6%	7.6M	✓
AlexNet-Orig [26]	57.2%	61M	-

Table 2: Comparison with other methods on ImageNet-2012 using AlexNet as the base model. We are able to achieve comparable accuracies using only 9.7M parameters.

CIFAR-10 dataset. We delete a linear layer and remove dropouts from the VGG16 model. There are two differences between our code and the PyTorch ImageNet repository. Our ImageNet training code uses a batchsize of 128 for all experiments, and our AlexNet model uses BatchNorm layers to stabilize training, with a batchsize of 384.

We train all the models on a setup consisting of 10 Intel Xeon E5-2640 cores and 2 GeForce GTX 1080 Ti GPUs. All networks are trained from scratch. We model connections as random expanders for all experiments. The X-Conv layers do not have a bias. No dropouts were used, since our method inherently acts as a good regularizer.

## 5.4. Results

As described in Section 2, we compare with matrix compression techniques as well as the newer layer design techniques like DenseNets [23].

## 5.5. Comparison with Layer Design Techniques

Figures 3(a),(b) and (c) show the performance of X-Nets in comparison with current state-of-the-art compact architectures – DenseNets [23] and Wide Resnets [54]. We observe that we can achieve upto using only two-thirds of the parameter and runtime cost, keeping accuracy constant on CIFAR-10 and CIFAR-100 datasets. Similarly, we observe 15% fewer parameters keeping accuracy constant, and a 0.4% improvement in accuracy vice-versa using ResNet models on ImageNet dataset. DenseNets consistently give a 3% drop in accuracy with 2x compression on ImageNet dataset (Tabulated in Appendix). We use the Wide-DenseNets<sup>4</sup> as base models on CIFAR datasets, for practical purposes. These results empirically validate our hypothesis - that X-Conv layers are able to efficiently model convolutional layers and that modeling connections as expander graphs retains accuracy with a significant reduction in the number of parameters.

## 5.6. Comparison with Compression Techniques

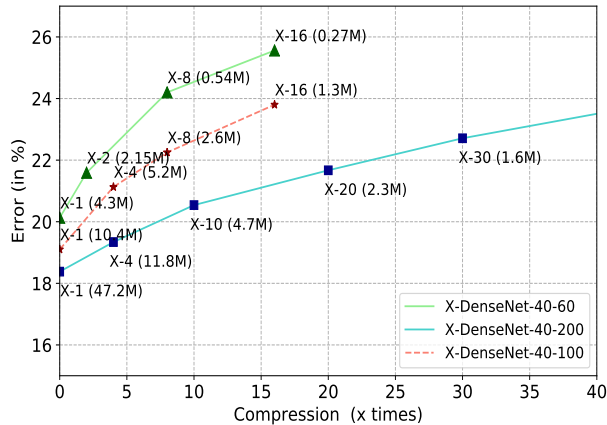
In Table 1, we compare the performance of VGG16 X-Net against the current state-of-the-art pruning techniques. We see that we achieve accuracies comparable to the original VGG16 model, with 9x-13x fewer parameters. In Table 2 we present our results on AlexNet trained on ImageNet dataset. We achieve comparable accuracy to AlexNet model using only 9.7M parameters, which is comparable to SELLs. Note that SELLs [34, 50] exclusively optimize the linear layers, unlike a generic approach as ours. Additionally, pruning techniques used by Hao *et al.* [29] and Zhuang *et al.* [32] require significantly longer training times, involve multiple passes across the whole training process, and achieve the specified model compression only after training, as explained in the related work (see Section 2).

In contrast, our model can be trained in a simple, fast, and efficient fashion. We simply initialize the compact X-Net model and train it as we train the original VGG16 or AlexNet model. In addition, we have the ability to leverage fast convolution algorithms to reduce both train and test time. This advantage, as we will see in the next section 5.7, enables us to train significantly wider and deeper networks. An advantage of developing a more efficient model for connecting neurons is that the model is less prone to over-fitting. Our method inherently works as a regularizer. Due to this fact, we do not need a dropout regularizer while training.

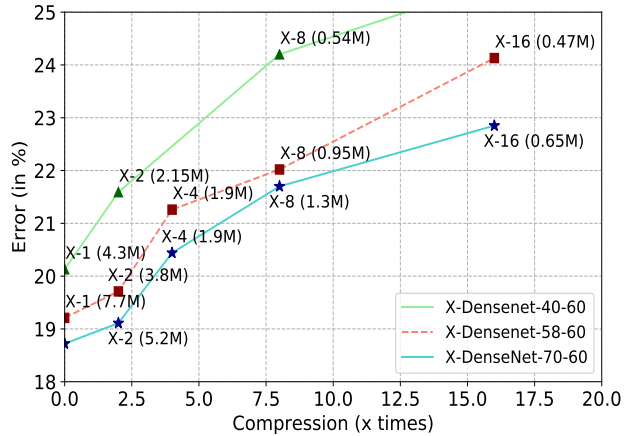
## 5.7. Training Wider and Deeper networks

Wide-Resnet [54] showed that increasing the width of ResNet [19] blocks is more effective than depth for improv-

<sup>4</sup><https://github.com/liuzhuang13/DenseNet#wide-densenet-for-better-timeaccuracy-and-memoryaccuracy-tradeoff>



(a) Effect of Width



(b) Effect of Depth

Figure 4: We present the effect of increasing the compression by using significantly wider and deeper networks in this figure. Every datapoint is X-C specified along with the number of parameters, C being the compression factor. We show that training wider or deeper networks along with more compression using X-Nets achieve better accuracies with upto two-thirds of the total parameter and FLOPs on CIFAR-100 dataset.

ing accuracy efficiently. In that spirit, DenseNet [23] formulated Wide-DenseNets<sup>5</sup>, which offered a better accuracy-memory-time trade-off. In these DenseNet models, the depth is kept constant at 40, and the growth rate is increased from 24 to 60 in steps of 12. We further increase the growth rate to 100, and then 200, to get "Wider" DenseNets. Similarly, we get deeper networks by increasing the depth of DenseNet-40-60 to 70 in steps of 18 and 12. Using X-Nets, Wide-DenseNets could only be compressed by a factor of 2 or 4, owing to their already compact nature. However, we can study the effectiveness of expander graph constructions on these Wider networks using CIFAR-100 dataset.

Figure 4 (a) shows that expander graph constructions are able to model connections between the layers of networks even at compression rates of 50x with only 4.5% drop in accuracy, enabling us to train significantly wider networks efficiently. For example, it can effectively model Wider DenseNet-40-200, an efficient architecture with over 47M parameters with just 1.6M parameters, a further 30x compression ratio. The slope of the curves indicate that wider network suffer lesser penalty with compression, indicating that expander graph modeling is highly effective on wider X-Nets.

We also investigate the performance when increasing the depth D of the networks. We trained 58 and 70 layered X-DenseNet-D-60 model. Figure 4 (b) shows that the we are able to achieve improved accuracies with the same number of parameters while training deeper expander networks. Expander graphs were able to model the model connections between the layers of networks even at compression rates of 8-16x without a drastic drop in accuracy, given the net-

works were still very compact (in  $\leq 10M$  parameter range). The drop of accuracy over compression rate was lower for deeper networks, indicating that our approach is more effective with the increase in depth. The interesting second observation from Figure 4(b) is that X-DenseNet-70-60 significantly outperforms X-DenseNet-58-60 with fewer parameters for a wide range of k values. It indicates that Expander Graphs modeling enables us to scale up training to deeper and wider networks retaining similar parameters efficiently.

## 6. Conclusion

We proposed a new network layer architecture for deep networks using expander graphs that give strong theoretical guarantees on connectivity. The resulting architecture (X-Net) is shown to be highly efficient in terms of both computational requirements and model size. In addition to being compact and computationally efficient, the connectivity properties of the network allows us to achieve significant improvements over the state-of-the-art architectures in performance on a parameter or run-time budget. In short, we show that the use of principled approaches that sparsify a model while maintaining global information flows can help in developing efficient deep networks.

To the best of our knowledge, this is the first attempt at using theoretical results from graph theory in modeling connectivity to improve deep network architectures. We believe that the field of deep networks can gain significantly from other similar explorations.

<sup>5</sup><https://github.com/liuzhuang13/DenseNet#wide-densenet-for-better-timeaccuracy-and-memoryaccuracy-tradeoff>



## 7. Acknowledgements

We would like to thank the *Kohli Center on Intelligent Systems at IIIT Hyderabad* for partial support of this work. We thank Sri Aurobindo Munagala, Saujas V S and Vishal Batchu for their helpful suggestions.

## References

- [1] N. Alon and Y. Roichman. Random cayley graphs and expanders. *Random Struct. Algorithms*, 5:271–285, 1994. [3](#), [11](#)
- [2] H. Bagherinezhad, M. Rastegari, and A. Farhadi. Lcnn: Lookup-based convolutional neural network. *CVPR*, 2017. [2](#)
- [3] C. Blundell, J. Cornebise, K. Kavukcuoglu, and D. Wierstra. Weight uncertainty in neural networks. *ICML*, 2015. [1](#), [2](#)
- [4] W. Chen, J. Wilson, S. Tyree, K. Weinberger, and Y. Chen. Compressing neural networks with the hashing trick. In *ICML*, pages 2285–2294, 2015. [1](#), [2](#), [3](#)
- [5] Y. Cheng, F. X. Yu, R. S. Feris, S. Kumar, A. Choudhary, and S.-F. Chang. An exploration of parameter redundancy in deep networks with circulant projections. In *CVPR*, pages 2857–2865, 2015. [1](#), [7](#)
- [6] F. Chollet. Xception: Deep learning with depthwise separable convolutions. *CVPR*, 2017. [1](#), [2](#)
- [7] N. Cohen, O. Sharir, and A. Shashua. Deep simnets. In *CVPR*, pages 4782–4791, 2016. [1](#), [3](#)
- [8] M. D. Collins and P. Kohli. Memory bounded deep convolutional networks. *arXiv preprint arXiv:1412.1442*, 2014. [7](#)
- [9] M. Courbariaux and Y. Bengio. Binarynet: Training deep neural networks with weights and activations constrained to +1 or -1. *ICML*, 2016. [2](#)
- [10] B. Dai, B. Xie, N. He, Y. Liang, A. Raj, M.-F. F. Balcan, and L. Song. Scalable kernel methods via doubly stochastic gradients. In *NIPS*, pages 3041–3049, 2014. [1](#)
- [11] J. Deng, W. Dong, R. Socher, L.-J. Li, K. Li, and L. Fei-Fei. Imagenet: A large-scale hierarchical image database. In *CVPR 2009*, pages 248–255. IEEE, 2009. [5](#)
- [12] M. Denil, B. Shakibi, L. Dinh, N. de Freitas, et al. Predicting parameters in deep learning. In *NIPS*, pages 2148–2156, 2013. [1](#)
- [13] E. L. Denton, W. Zaremba, J. Bruna, Y. LeCun, and R. Fergus. Exploiting linear structure within convolutional networks for efficient evaluation. In *NIPS*, pages 1269–1277, 2014. [1](#)
- [14] M. Figurnov, A. Ibraimova, D. P. Vetrov, and P. Kohli. Perforatedcnns: Acceleration through elimination of redundant convolutions. In *NIPS*, pages 947–955, 2016. [1](#)
- [15] Y. Gong, L. Liu, M. Yang, and L. Bourdev. Compressing deep convolutional networks using vector quantization. *arXiv preprint arXiv:1412.6115*, 2014. [1](#)
- [16] Y. Guo, A. Yao, and Y. Chen. Dynamic network surgery for efficient dnns. In *NIPS*, pages 1379–1387, 2016. [2](#), [7](#)
- [17] S. Han, H. Mao, and W. J. Dally. Deep compression: Compressing deep neural networks with pruning, trained quantization and huffman coding. *International Conference on Learning Representations (ICLR)*, 2016. [1](#), [2](#), [7](#)
- [18] S. Han, J. Pool, J. Tran, and W. Dally. Learning both weights and connections for efficient neural network. In *NIPS*, pages 1135–1143, 2015. [1](#)
- [19] K. He, X. Zhang, S. Ren, and J. Sun. Deep residual learning for image recognition. In *CVPR*, pages 770–778, June 2016. [1](#), [2](#), [6](#), [7](#)
- [20] Y. He, X. Zhang, and J. Sun. Channel pruning for accelerating very deep neural networks. *CVPR*, 2017. [2](#)
- [21] S. Hoory, N. Linial, and A. Wigderson. Expander graphs and their applications. *BULL. AMER. MATH. SOC.*, 43(4):439–561, 2006. [2](#), [3](#), [11](#)
- [22] A. G. Howard, M. Zhu, B. Chen, D. Kalenichenko, W. Wang, T. Weyand, M. Andreetto, and H. Adam. Mobilenets: Efficient convolutional neural networks for mobile vision applications. *arXiv preprint arXiv:1704.04861*, 2017. [1](#), [2](#), [13](#)
- [23] G. Huang, Z. Liu, K. Q. Weinberger, and L. van der Maaten. Densely connected convolutional networks. *CVPR*, 2017. [2](#), [6](#), [7](#), [8](#)
- [24] F. N. Iandola, S. Han, M. W. Moskewicz, K. Ashraf, W. J. Dally, and K. Keutzer. Squeezenet: Alexnet-level accuracy with 50x fewer parameters and <0.5mb model size. *ICLR*, 2017. [1](#), [2](#)
- [25] A. Krizhevsky and G. Hinton. Learning multiple layers of features from tiny images. 2009. [5](#)
- [26] A. Krizhevsky, I. Sutskever, and G. E. Hinton. Imagenet classification with deep convolutional neural networks. In *NIPS*, pages 1097–1105, 2012. [5](#), [7](#)
- [27] V. Lebedev and V. Lempitsky. Fast convnets using group-wise brain damage. In *CVPR*, pages 2554–2564, 2016. [2](#)
- [28] Y. LeCun, J. S. Denker, and S. A. Solla. Optimal brain damage. In *NIPS*, pages 598–605. 1990. [1](#)
- [29] H. Li, A. Kadav, I. Durdanovic, H. Samet, and H. P. Graf. Pruning filters for efficient convnets. *ICLR*, 2017. [2](#), [7](#)
- [30] M. Lin, Q. Chen, and S. Yan. Network in network. *ICLR*, 2014. [2](#)
- [31] B. Liu, M. Wang, H. Foroosh, M. Tappen, and M. Pensky. Sparse convolutional neural networks. In *CVPR*, pages 806–814, 2015. [1](#), [2](#)
- [32] Z. Liu, J. Li, Z. Shen, G. Huang, S. Yan, and C. Zhang. Learning efficient convolutional networks through network slimming. *ICCV*, 2017. [2](#), [6](#), [7](#)
- [33] M. Masana, J. van de Weijer, L. Herranz, A. D. Bagdanov, and J. MALvarez. Domain-adaptive deep network compression. *network*, 16:30, 2017. [2](#)
- [34] M. Moczulski, M. Denil, J. Appleyard, and N. de Freitas. Acdc: A structured efficient linear layer. *ICLR*, 2016. [1](#), [3](#), [7](#)
- [35] P. Molchanov, S. Tyree, T. Karras, T. Aila, and J. Kautz. Pruning convolutional neural networks for resource efficient inference. *ICLR*, 2017. [2](#)
- [36] A. Novikov, D. Podoprikin, A. Osokin, and D. P. Vetrov. Tensorizing neural networks. In *NIPS*, pages 442–450, 2015. [2](#)
- [37] M. Rastegari, V. Ordonez, J. Redmon, and A. Farhadi. Xnornet: Imagenet classification using binary convolutional neural networks. In *ECCV*, 2016. [2](#)
- [38] T. N. Sainath, B. Kingsbury, V. Sindhvani, E. Arisoy, and B. Ramabhadran. Low-rank matrix factorization for deep

- neural network training with high-dimensional output targets. In *ICASSP*, pages 6655–6659. IEEE, 2013. 1, 2, 3
- [39] S. Scardapane, D. Comminiello, A. Hussain, and A. Uncini. Group sparse regularization for deep neural networks. *Neurocomputing*, 241:81–89, 2017. 2
- [40] K. Simonyan and A. Zisserman. Very deep convolutional networks for large-scale image recognition. *CoRR*, abs/1409.1556, 2014. 1, 5, 7
- [41] D. A. Spielman. Spectral graph theory and its applications. In *FOCS 2007*, pages 29–38, Oct 2007. 2
- [42] S. Srinivas and R. V. Babu. Data-free parameter pruning for deep neural networks. *BMVC*, 2015. 2
- [43] S. Srinivas, A. Subramanya, and R. V. Babu. Training sparse neural networks. In *(CVPRW)*, pages 455–462. IEEE, 2017. 2, 7
- [44] C. Szegedy, W. Liu, Y. Jia, P. Sermanet, S. Reed, D. Anguelov, D. Erhan, V. Vanhoucke, and A. Rabinovich. Going deeper with convolutions. In *CVPR*, pages 1–9, June 2015. 1, 2
- [45] S. P. Vadhan. Pseudorandomness. *Foundations and Trends in Theoretical Computer Science*, 7(13):1–336, 2012. 2, 3, 11
- [46] W. Wen, C. Wu, Y. Wang, Y. Chen, and H. Li. Learning structured sparsity in deep neural networks. In *NIPS*, pages 2074–2082. 2016. 2
- [47] A. G. Wilson, Z. Hu, R. Salakhutdinov, and E. P. Xing. Deep kernel learning. In *Artificial Intelligence and Statistics*, pages 370–378, 2016. 1, 3
- [48] J. Wu, C. Leng, Y. Wang, Q. Hu, and J. Cheng. Quantized convolutional neural networks for mobile devices. In *CVPR*, pages 4820–4828, 2016. 2
- [49] J. Xue, J. Li, and Y. Gong. Restructuring of deep neural network acoustic models with singular value decomposition. In *Interspeech*, pages 2365–2369, 2013. 1
- [50] Z. Yang, M. Moczulski, M. Denil, N. de Freitas, A. Smola, L. Song, and Z. Wang. Deep fried convnets. In *CVPR*, pages 1476–1483, 2015. 1, 3, 7
- [51] J. Yoon and S. J. Hwang. Combined group and exclusive sparsity for deep neural networks. In *ICML*, pages 3958–3966, 2017. 2
- [52] F. Yu and V. Koltun. Multi-scale context aggregation by dilated convolutions. *ICLR*, 2016. 1
- [53] X. Yu, T. Liu, X. Wang, and D. Tao. On compressing deep models by low rank and sparse decomposition. In *CVPR*, pages 7370–7379, 2017. 7
- [54] S. Zagoruyko and N. Komodakis. Wide residual networks. *BMVC*, 2016. 2, 7
- [55] X. Zhang, X. Zhou, M. Lin, and J. Sun. Shufflenet: An extremely efficient convolutional neural network for mobile devices. *arXiv preprint arXiv:1707.01083*, 2017. 1, 13
- [56] H. Zhou, J. M. Alvarez, and F. Porikli. Less is more: Towards compact cnns. In *ECCV*, pages 662–677. Springer, 2016. 2, 7
- [57] S. Zhou, Y. Wu, Z. Ni, X. Zhou, H. Wen, and Y. Zou. Dorefanet: Training low bitwidth convolutional neural networks with low bitwidth gradients. *ICLR*, 2016. 2
- [58] C. Zhu, S. Han, H. Mao, and W. J. Dally. Trained ternary quantization. *ICLR*, 2017. 2

## 8. Appendix

This appendix provides formal proofs for the theorems stated in Section 3 of the main paper. We also include tabulation of results of Figure 3 and 4, alongside additional results that could not be added in the paper due to space constraints.

### A. Explicit Expanders

In this section, we will give details about some properties of expander graphs that are required for proving Theorems 1 and 2. Expander graphs are characterized by the spectral gap, which in turn implies the connectivity properties listed in Section 3.1. Many constructions of expander graphs have been explored in the past (see [21]). We will be using a construction that is comparatively easy to describe and implement. We will be considering Cayley graphs, which are obtained from the theory of finite Fields/Groups. The vertex set of such graphs is a group and the edges are defined by addition operation on the vertices. Also we will be describing expanders that are simple undirected graphs. Given an undirected graph  $G = (V, E)$ , we can obtain a bipartite expander  $G = (V, V', E)$ , by making a copy of the vertices  $V$  on the other side and adding edges according to  $E$ .

#### A.1. Cayley Expander

Let  $V$  be a group under an operation  $+$  and let  $H \subset V$  be a set of generators of the group  $V$ . The Cayley graph defined by  $V, H$  is the graph with vertex set  $V$  and the edges  $E = \{(x, x + h) : h \in H\}$ . For our construction, we will consider the group  $\{0, 1\}^n$  under coordinate-wise XOR operations. For  $H \subset \{0, 1\}^n$ , the Cayley graph defined by  $H$  is  $|H|$ -regular. It is a well-known result in spectral graph theory that there are set of generators  $H$ , for which the Cayley graph defined by  $\{0, 1\}^n, H$  forms an expander with spectral gap  $\gamma$ .

**Theorem 1** (Alon, Roichman, Proposition 4 [1]). *For every  $\epsilon$ , there exists explicit  $H \subset \{0, 1\}^n$  of size  $\leq O(n^2/\epsilon^2)$  such that the Cayley graph defined by  $\{0, 1\}^n, H$  is an expander with spectral gap  $\gamma = 1 - \epsilon$ .*

The properties given in Section 3.1 follows from the fact that expanders have a spectral gap (for proofs see [45]). For the sensitivity proofs, we need the following lemmas. The first lemma states that having a spectral gap, implies that all set of vertices of size  $\leq n/2$  expands.

**Lemma 1** (Theorem 4.6 [45]). *If  $G = (V, E)$  is an expander with spectral gap of  $\gamma$  then for every subset  $S \subset V$  of size  $\leq |V|/2$ , the size of the set of neighbors  $|N(S)| \geq (1 + \gamma)|S|$ .*

The next lemma is known as the expander mixing lemma, deals with the uniform connectivity properties of the expander.

**Lemma 2** (Lemma 4.15 [45]). *If  $G = (V, E)$  is an  $D$ -regular expander with spectral gap of  $\gamma$  then for every subset  $S, T \subset V$ ,*

$$|E(S, T) - D \cdot |S| \cdot |T|/n| \leq (1 - \gamma)\sqrt{|S| \cdot |T|}$$

where  $E(S, T)$  is the set of edges from  $S$  to  $T$ .

### B. Sensitivity in Expanders

In this section, we prove Theorem 1 and Theorem 2 using the properties described above along with the connectivity properties defined in Section 3.1 of the paper.

**Theorem 3** (Sensitivity of X-Nets). *Let  $n$  be the number of input as well as output nodes in the network and  $G_1, G_2, \dots, G_t$  be  $D$  regular bipartite expander graphs with  $n$  nodes on both sides. Then every output neuron is sensitive to every input in a Deep X-Linear Network defined by  $G_i$ 's with depth  $t = O(\log n)$ .*

*Proof.* For showing sensitivity, we show that for every pair of input and output  $(u, v)$ , there is a path in the X-Net with the  $i^{\text{th}}$  edge from the  $i^{\text{th}}$  graph. We use the expansion property of the expander graphs. Let  $N_1(u)$  be the set of neighbors of  $u$  in  $G_1$  and  $N_i(u)$  be the set of neighbors of  $N_{i-1}(u)$  in the graph  $G_i$ . Since each of the graphs are expanding  $|N_i(u)| \geq (1 + \gamma) \times |N_{i-1}(u)|$ , using Lemma 1. Since  $(1 + \gamma) > 1$ , we can obtain that for  $i = O(\log n)$ ,  $|N_i(u)| \geq n/2$ . Similarly we can start from  $v$  and define  $N_1(v)$  as the set of neighbors of  $v$  in  $G_t$  and  $N_i(v)$  be the set of neighbors of  $N_{i-1}(v)$  in the graph  $G_{n-i-1}$ . Due to the expansion property, for  $j = O(\log n)$ ,  $|N_j(v)| \geq n/2$ . Now we choose  $t = i + j = O(\log n)$  so that the  $i^{\text{th}}$  graph from 1 is the same as  $j + 1^{\text{th}}$  graph from  $t$ . Then we will have that  $N_i(u) \cap N_j(v) \neq \emptyset$ . That is there is some vertex in the  $i^{\text{th}}$  graph that is both connected to  $u$  and  $v$ , which implies that there is a path from  $u$  to  $v$ .  $\square$

**Theorem 4** (Mixing in Deep Expander Networks). *Let  $n$  be the number of input as well as output nodes in the network and  $G_1, G_2, \dots, G_t$  be  $D$  regular bipartite expander graphs with  $n$  nodes on both sides. Let  $S, T$  be subsets of input and output nodes in the X-Linear Network defined by the  $G_i$ 's. The number of paths between  $S$  and  $T$  is  $\approx D|S||T|/n$*

*Proof.* First we prove the theorem for the case when  $G_1 = G_2 \dots = G_t = G$ . Note that for  $t = 1$ , the theorem is same as the expander mixing lemma (Lemma 2). For  $t > 1$ , consider the graph of  $t$  length paths denoted by  $G^t$ . An edge in this graph denotes that there is a path of length  $t$  in  $G$ . Observe that the adjacency matrix of  $G^t$  is given by the  $t$ th power of the adjacency matrix of  $G$  and hence the spectral gap of  $G^t$ ,  $\gamma_t = \gamma^t$ . Now applying the expander mixing lemma on  $G^t$  (Lemma 2), proves the theorem.

AlexNet	Filter Shape	Filter Shape (X-AlexNet-1)	Filter Shape (X-AlexNet-2)
Conv2d	64 x 3 x 11 x 11	64 x 3 x 11 x 11	64 x 3 x 11 x 11
Conv2d	192 x 64 x 5 x 5	192 x 64 x 5 x 5	192 x 64 x 5 x 5
Conv2d	384 x 192 x 3 x 3	384 x 192 x 3 x 3	384 x 192 x 3 x 3
Conv2d	256 x 384 x 3 x 3	256 x 384 x 3 x 3	256 x 384 x 3 x 3
Conv2d	256 x 256 x 3 x 3	256 x 256 x 3 x 3	256 x 256 x 3 x 3
Linear	9216 x 4096	1024 x 4096	512 x 4096
Linear	4096 x 4096	512 x 4096	512 x 4096
Linear	4096 x 1000	1024 x 1000	1024 x 1000

Table 3: Filter sizes for the AlexNet model. Notice the filter sizes of the linear layers of the original model has  $|V| \times |U|$  parameters, whereas X-AlexNet models have  $|V| \times D$  parameters. Note that  $D \ll |U|$  as stated in Section 3.2. Hence, expander graphs model connections in linear layers (X-Linear) effectively.

VGG	Filter Shape	Filter Shape (X-VGG16-1)	Filter Shape (X-VGG16-2)
Conv2d	64 x 3 x 3 x 3	64 x 3 x 3 x 3	64 x 3 x 3 x 3
Conv2d	64 x 64 x 3 x 3	64 x 64 x 3 x 3	64 x 64 x 3 x 3
Conv2d	128 x 64 x 3 x 3	128 x 64 x 3 x 3	128 x 64 x 3 x 3
Conv2d	128 x 128 x 3 x 3	128 x 64 x 3 x 3	128 x 64 x 3 x 3
Conv2d	256 x 128 x 3 x 3	256 x 32 x 3 x 3	256 x 16 x 3 x 3
Conv2d	256 x 256 x 3 x 3	256 x 32 x 3 x 3	256 x 16 x 3 x 3
Conv2d	256 x 256 x 3 x 3	256 x 32 x 3 x 3	256 x 16 x 3 x 3
Conv2d	512 x 256 x 3 x 3	512 x 32 x 3 x 3	512 x 16 x 3 x 3
Conv2d	512 x 512 x 3 x 3	512 x 32 x 3 x 3	512 x 16 x 3 x 3
Conv2d	512 x 512 x 3 x 3	512 x 32 x 3 x 3	512 x 16 x 3 x 3
Conv2d	512 x 512 x 3 x 3	512 x 32 x 3 x 3	512 x 16 x 3 x 3
Conv2d	512 x 512 x 3 x 3	512 x 32 x 3 x 3	512 x 16 x 3 x 3
Conv2d	512 x 512 x 3 x 3	512 x 32 x 3 x 3	512 x 16 x 3 x 3
Linear	512 x 512	128 x 512	128 x 512
Linear	512 x 10	512 x 10	512 x 10

Table 4: Filter sizes for the VGG-16 model on CIFAR-10 dataset. The filter sizes given are  $|V| \times |U| \times c \times c$  in original VGG network,  $|V| \times D \times c \times c$  in our X-VGG16 models. Note that  $D \ll |U|$  as stated in Section 3.2. Hence, expander graphs model connections in Convolutional layers (X-Conv) effectively.

For the case when the graph  $G_i$ 's are different, let  $\gamma_{\min}$  be the minimal spectral gap among the graphs. Since all the graphs are  $D$ -regular, the largest eigenvector is the all ones vector with eigenvalue  $D$  for all the graphs. The eigenvector corresponding to second largest eigenvalue can be different for each graph, but they are orthogonal to the all ones vector. Hence the spectral gap of the  $t$  length path graph  $G$  is at least  $\gamma_{\min}^t$ . Finally we apply the expander mixing lemma on  $G^t$  to prove the theorem.  $\square$

## C. Model Details

We discuss the model structures in detail, along with tabulated values of size and flops of various architectures pre-

Model	Accuracy	#Params (in M)	#FLOPs (in 100M)
CIFAR10			
X-DenseNetBC-2-40-24	<b>94.83%</b>	<b>0.4M</b>	<b>1.44</b>
DenseNetBC-40-24	94.79%	0.7M	2.88
X-DenseNetBC-2-40-36	94.98%	0.75M	3.24
X-DenseNetBC-2-40-48	<b>95.48%</b>	<b>1.4M</b>	<b>5.75</b>
DenseNetBC-40-36	95.26%	1.5M	6.47
X-DenseNetBC-2-40-60	<b>95.71%</b>	<b>2.15M</b>	<b>8.98</b>
DenseNetBC-40-48	95.64%	2.8M	11.50
DenseNetBC-40-60	95.91%	4.3M	17.96
CIFAR100			
X-DenseNetBC-2-40-24	74.37%	0.4M	1.44
DenseNetBC-40-24	76.05%	0.7M	2.88
X-DenseNetBC-2-40-36	<b>76.69%</b>	<b>0.75M</b>	<b>3.24</b>
DenseNetBC-40-36	77.84%	1.5M	6.47
X-DenseNetBC-2-40-60	78.53%	2.15M	8.98
X-DenseNetBC-4-70-60	<b>79.56%</b>	<b>2.6M</b>	<b>10.26</b>
DenseNetBC-40-48	79.03%	2.8M	11.50
DenseNetBC-40-60	79.87%	4.3M	17.96
X-DenseNetBC-2-70-60	80.89%	5.18M	20.52
DenseNetBC-70-60	81.28%	10.36M	41.05

Table 5: Results obtained on the state-of-the-art models on CIFAR-10 and CIFAR-100 datasets, ordered by FLOPs per model. X-Nets give significantly better accuracies with corresponding DenseNet models in the same limited computational budget and correspondingly significant parameter and FLOP reduction for models with similar accuracy.

sented as graphs in the main paper in Figure 3 and 4.

### C.1. Filter structure of AlexNet and VGG

In Tables 3 and 4, the detailed layer-wise filter structure is tabulated as stated in Section 5.2 of the paper. We compare the sizes of input channels between the filters, and show that with X-Conv and X-Linear layers, we can train models effectively even with upto 32x and 18x times smaller filters in input dimension in VGG16 and AlexNet models respectively. Hence, modeling connections as weighted adjacency matrix of an Expander graph is an effective method to model connections between neurons, producing highly efficient X-Nets.

### C.2. Results

As stated in Section 5.2, Tables 5 and 6 presented below give the detailed accuracy, parameters and FLOPs of models displayed in the Figure 3 in the paper. Details of other models are also provided in the same table, which could not be displayed in the paper due to lack of space.

Table 5 displays the performance of X-DenseNet models on the CIFAR-10 and CIFAR-100 datasets. If we compare models that have similar number of parameters, we achieve around 0.2% and 0.6% increase in accuracy over DenseNet-BC models on CIFAR-10 and CIFAR-100 datasets respectively. In the same manner, we can achieve upto using only

Model	Accuracy	#Params	#FLOPs
ResNet		(in M)	(in 100M)
X-ResNet-2-34	69.23%	11M	35
X-ResNet-2-50	<b>72.85%</b>	<b>13M</b>	<b>40</b>
ResNet-34	71.66%	22M	70
X-ResNet-2-101	<b>74.87%</b>	<b>22.5M</b>	<b>80</b>
ResNet-50	74.46%	26M	80
ResNet-101	75.87%	45M	160
DenseNetBC			
MobileNet [22]	70.6%	4.2M	5.7 <sup>6</sup>
ShuffleNet [55]	70.9%	5M	5.3 <sup>7</sup>
X-DenseNetBC-2-121	<b>70.5%</b>	<b>4M</b>	28
X-DenseNetBC-2-169	71.7%	7M	33
X-DenseNetBC-2-201	72.5%	10M	43
X-DenseNetBC-2-161	<b>74.3%</b>	14.3M	<b>55</b>
DenseNetBC-121	73.3%	8M	55
DenseNetBC-169	74.8%	14M	65
DenseNetBC-201	75.6%	20M	85
DenseNetBC-161	76.3%	28.5M	110

Table 6: Results obtained on the state-of-the-art models on ImageNet dataset, ordered by FLOPs. We also observe that X-DenseNetBC models outperform ResNet and X-ResNet models in both compression, parameters and FLOPs and achieve comparable accuracies with the highly efficient MobileNets and ShuffleNets in the same parameter budget, albeit with much higher FLOPs due to architectural constraints.

two-thirds of the parameter and runtime cost cost respectively, keeping accuracy constant on CIFAR-10 and CIFAR-100 datasets as stated in the paper.

Similarly, Table 6 displays the performance of X-ResNet and X-DenseNet models on the ImageNet datasets. We can observe that we achieve around 3.2% and 1% increase in accuracy over ResNet and DenseNet-BC models in the same computational budget. Also, we can observe that we require approximately 15% less FLOPs for achieving similar accuracies over DenseNet models and 15% less parameters for achieving similar accuracies over the ResNet model respectively as stated in the paper. We also observe that X-DenseNetBC models outperform ResNet and X-ResNet models in both compression, parameters and FLOPs and achieve comparable accuracies with MobileNets [22] and ShuffleNets [55] in the same parameter budget, albeit with much higher computational cost due to architectural constraints.

Table 7 displays accuracies, parameters and FLOPs of all the wider and deeper networks trained on CIFAR-100 dataset as discussed in Section 5.7. They are listed in increasing compression order from DensenetBC (1x) to the highest compressed X-DenseNet. The figure indicates that Expander Graphs modeling can scale up to high compression ratios without drastic drops in accuracies, enabling us

Model	Accuracy	#Params	#FLOPs
Wider		(in M)	(in 100M)
DenseNetBC-40-60	79.87%	4.3M	17.96
X-DenseNetBC-2-40-60	78.53%	2.15M	8.98
X-DenseNetBC-4-40-60	77.54%	1.08M	4.49
X-DenseNetBC-8-40-60	75.29%	0.54M	2.24
X-DenseNetBC-16-40-60	74.44%	0.27M	1.12
DenseNetBC-40-100	80.9%	11.85M	49.85
X-DenseNetBC-4-40-100	78.87%	2.9M	12.46
X-DenseNetBC-8-40-100	77.75%	1.48M	6.23
X-DenseNetBC-16-40-100	76.2%	0.74M	3.12
DenseNetBC-40-200	81.62%	47.19M	199.28
X-DenseNetBC-4-40-200	80.66%	11.79M	49.82
X-DenseNetBC-10-40-200	79.46%	4.71M	19.93
X-DenseNetBC-20-40-200	78.33%	2.3M	9.96
X-DenseNetBC-30-40-200	77.29%	1.6M	6.64
X-DenseNetBC-50-40-200	75.7%	0.9M	3.99
X-DenseNetBC-80-40-200	73.26%	0.5M	2.49
Deeper			
DenseNetBC-40-60	79.87%	4.3M	17.96
X-DenseNetBC-2-40-60	78.53%	2.15M	8.98
X-DenseNetBC-8-40-60	77.54%	0.54M	2.24
X-DenseNetBC-16-40-60	75.29%	0.27M	1.12
DenseNetBC-58-60	80.79%	7.66M	30.96
X-DenseNetBC-2-58-60	80.29%	3.83M	15.48
X-DenseNetBC-4-58-60	78.74%	1.9M	7.74
X-DenseNetBC-8-58-60	77.98%	0.95M	3.87
X-DenseNetBC-16-58-60	75.87%	0.47M	1.93
DenseNetBC-70-60	81.28%	10.36M	41.05
X-DenseNetBC-2-70-60	80.89%	5.18M	20.52
X-DenseNetBC-4-70-60	79.56%	2.6M	10.26
X-DenseNetBC-8-70-60	77.48%	1.3M	5.13
X-DenseNetBC-16-70-60	77.23%	0.65M	2.57

Table 7: We display accuracies, parameters and FLOPs of all the wider and deeper networks on CIFAR-100 listed in increasing compression order. This proves that efficiently designing layers like X-Conv and X-Linear allows us to train wider and deeper networks frugally.

to train deeper and wider networks retaining similar FLOPs and parameters effectively. We believe this modeling can open up a interesting exploration of training significantly deeper and wider range of models, unlike the current compression techniques as X-Nets are highly compressed networks since definition.

### C.2.1 Additional Training Details

All models in the plot were trained from the ImageNet code available on Pytorch Official repository including the original DenseNet and ResNet models. Note that this training code is common for all models in the repository and not fine-tuned to any specific model like ResNet or DenseNet. Hence the accuracies we report is slightly lower that those reported using model-specific training code. However, note that we have used the same code for training both the original models and the expander versions of these models.

Hence the comparison is a fair one. Same is true with the AlexNet model. Note that we use the original AlexNet architecture, and not CaffeNet. In contrast, training with fine-tuned code is expected to give a 1-2% improvement over MobileNets in Table 6. Training schedules suited to X-Nets, hyper-parameter tuning, Activation layers tailored to X-Nets could further improve the accuracies. Overall, we believe that investigating training methods for X-Nets has a lot of potential for improving their performance.